AMERICAN SOCIETY FOR MICROBIOLOGY | Journal of Virology®

VIRUS-CELL INTERACTIONS

Host Tumor Suppressor p18^{INK4c} Functions as a Potent Cell-Intrinsic Inhibitor of Murine Gammaherpesvirus 68 Reactivation and Pathogenesis

Brian F. Niemeyer,[a] Lauren M. Oko,[a] Eva M. Medina,[a] Darby G. Oldenburg,[b] Douglas W. White,[b] Carlyne D. Cool,[c] Eric T. Clambey,[d] Linda F. van Dyk[a]

[a]Immunology and Microbiology Department, University of Colorado Denver School of Medicine, Aurora, Colorado, USA

[b]Gundersen Health System, La Crosse, Wisconsin, USA

[c]Department of Pathology and Division of Pulmonary Sciences and Critical Care Medicine, School of Medicine, University of Colorado Anschutz Medical Campus, Aurora, Colorado, USA

[d]Department of Anesthesiology, University of Colorado Anschutz Medical Campus, Aurora, Colorado

ABSTRACT Gammaherpesviruses are common viruses associated with lifelong infection and increased disease risk. Reactivation from latency aids the virus in maintaining infection throughout the life of the host and is responsible for a wide array of disease outcomes. Previously, we demonstrated that the virus-encoded cyclin (v-cyclin) of murine gammaherpesvirus 68 (γHV68) is essential for optimal reactivation from latency in normal mice but not in mice lacking the host tumor suppressor p18^{INK4c} (p18). Whether p18 plays a cell-intrinsic or -extrinsic role in constraining reactivation remains unclear. Here, we generated recombinant viruses in which we replaced the viral cyclin with the cellular p18^{INK4c} gene (p18KI) for targeted expression of p18, specifically within infected cells. We find that the p18KI virus is similar to the cyclin-deficient virus (cycKO) in lytic infection, establishment of latency, and infected cell reservoirs. While the cycKO virus is capable of reactivation in p18-deficient mice, expression of p18 from the p18KI virus results in a profound reactivation defect. These data demonstrate that p18 limits reactivation within latently infected cells, functioning in a cell-intrinsic manner. Further, the p18KI virus showed greater attenuation of virus-induced lethal pneumonia than the cycKO virus, indicating that p18 could further restrict γHV68 pathogenesis even in p18-sufficient mice. These studies demonstrate that host p18 imposes the requirement for the viral cyclin to reactivate from latency by functioning in latently infected cells and that p18 expression is associated with decreased disease, thereby identifying p18 as a compelling host target to limit chronic gammaherpesvirus pathogenesis.

IMPORTANCE Gammaherpesviruses are ubiquitous viruses associated with multiple malignancies. The propensity to cycle between latency and reactivation results in an infection that is never cleared and often difficult to treat. Understanding the balance between latency and reactivation is integral to treating gammaherpesvirus infection and associated disease outcomes. This work characterizes the role of a novel inhibitor of reactivation, host p18^{INK4c}, thereby bringing more clarity to a complex process with significant outcomes for infected individuals.

KEYWORDS gammaherpesvirus, p18, reactivation, viral cyclin

Herpesviruses have coevolved with their respective hosts for millions of years and are uniquely adapted to achieve successful propagation by infection programs that are highly attuned to their host cells. The gammaherpesviruses (γHV) are a subgroup of herpesviruses known for their lifelong persistence in lymphocytes and for

Received 9 September 2017 **Accepted** 9 December 2017

Accepted manuscript posted online 3 January 2018

Citation Niemeyer BF, Oko LM, Medina EM, Oldenburg DG, White DW, Cool CD, Clambey ET, van Dyk LF. 2018. Host tumor suppressor p18^{INK4c} functions as a potent cell-intrinsic inhibitor of murine gammaherpesvirus 68 reactivation and pathogenesis. J Virol 92:e01604-17. https://doi.org/10.1128/JVI.01604-17.

Editor Richard M. Longnecker, Northwestern University

Address correspondence to Linda F. van Dyk, Linda.VanDyk@ucdenver.edu.

malignancies associated with chronic infection. These viruses include the human pathogens Epstein-Barr virus (EBV) and Kaposi's sarcoma-associated herpesvirus (KSHV) and the small-animal model virus, gammaherpesvirus 68 (γHV68) (1, 2). The life cycles of these viruses are characterized by distinct phases. First, during a primary infection, γHV undergo lytic replication, a highly inflammatory and immunogenic process characterized by full viral gene expression and production of new infectious virus. These viruses also establish latent infection, a process critical to lifelong infection that is marked by retention of the viral genome with a relative paucity of viral transcription and translation and little to no production of new virus. While primary infection and spread involves a number of different cell types, latent infection is found primarily within lymphocytes (2, 3). Critical to lifelong infection and to transmission is the transition from the repressed latent state to lytic replication, termed reactivation from latency. In addition to being required for lifelong infection and spread, virus reactivation is associated with chronic disease, including malignancies and inflammatory disease (4–6). Regulation of this critical transition is the subject of this study.

γHV use cyclins to promote reactivation from latency; EBV encodes genes that upregulate host D-type cyclins, whereas KSHV and γHV68 encode viral homologues of host D-type cyclins (v-cyclin) (1, 7–9). The v-cyclin gene is a latency-associated gene which is dispensable for virus replication and establishment of latency but critical for reactivation from latency, such that infection with viral cyclin-deficient γHV68 (cycKO) results in a 100-fold defect in reactivation frequency compared to wild-type (WT) virus infection (10, 11). Although the cycKO virus is severely defective in reactivation from latency, this virus is still capable of reactivating at low levels in immunocompromised hosts (12, 13). Given that the viral cyclins are homologues of host cyclins, host pathways may fulfill some v-cyclin requirement in reactivation at low levels. Indeed, our previous studies using a panel of γHV68 chimeric viruses demonstrated that host cyclin D3 was able to support reactivation from latency, although less efficiently than v-cyclin (14).

While the viral cyclin is required for reactivation across multiple strains of immunocompetent and immunodeficient mice, v-cyclin is dispensable for reactivation in mice lacking the host tumor suppressor and cyclin-dependent kinase inhibitor (CDKI) $p18^{INK4c}$ (p18) (15). This suggests a primary function of v-cyclin is to overcome a p18-dependent barrier to reactivation. p18 is a member of the INK4 family of cyclin-dependent kinase inhibitors/tumor suppressors that is uniquely required for generation of functional plasma cells and in other specific stages of lymphocyte development and differentiation (16–18). The capacity of p18 to repress γHV68 reactivation appears specific, in that a large panel of immune-deficient mice and mice deficient in other cell cycle inhibitors consistently exhibit a severe reactivation defect upon infection with the cycKO virus. Further, physiologic antagonism of p18 through cytokine signaling in normal p18-sufficient mice also results in decreased control of viral reactivation. This supports the model that the viral cyclin evolved to promote reactivation by antagonism of host p18 function. However, p18 plays tissue-specific roles in development and immunity and therefore could either regulate reactivation at a molecular level within infected cells or function on a systemic level by altering infected cell populations or immune control of infected cells. That is, whether p18 regulates reactivation via an indirect/systemic or cell-intrinsic way remains unknown.

Previous studies of γHV pathogenesis have been heavily reliant on bulk analysis of pooled populations of cells. To specifically identify infected cells, we used bacterial artificial chromosome (BAC) recombination to generate a series of mutant viruses in a β-lactamase (βla)-marked virus (as in Nealy et al. [19]). This β-lactamase-marked γHV68 (WT.βla) allows for effective identification of infected cells during lytic and latent infection by virtue of enzymatic amplification of gene expression from a fusion between the viral LANA and β-lactamase genes by *ex vivo* staining with a fluorescent cell-permeable substrate. Upon substrate cleavage by β-lactamase, a shift in fluorescence can identify individual infected cells (a surrogate marker for LANA gene expression) by flow cytometry. This β-lactamase marker allows us to reliably analyze infected cell populations at the single-cell level in late stages of latency (6+ weeks postinfec-

tion), time points which previously have been difficult to analyze using more conventional flow markers due to loss of signal. The enzymatic nature of β-lactamase allows for robust amplification of otherwise difficult-to-detect signals.

In this study, we designed new recombinant viruses to identify infected cell populations on a single-cell basis and to express p18 exclusively in infected cells. We demonstrate that p18 regulation of virus reactivation is not due to alterations in the establishment of latent infection or alterations in the composition of the infected cell population, and that p18 limits reactivation in a cell-intrinsic manner. Furthermore, our findings show that exogenous p18 expressed from the virus resulted in reduced pathogenesis in a model of viral pneumonia, with improved resolution to healthy lung homeostasis. These studies highlight a new regulatory hub for γHV reactivation and disease outcomes associated with γHV infection and elevate our understanding of γHV pathogenesis.

RESULTS

Generation and validation of β-lactamase-marked cyclin recombinant viruses. The γHV68 v-cyclin is critical for reactivation from latency in wild-type mice but is dispensable for reactivation in mice lacking the CDK inhibitor p18 (p18$^{-/-}$ mice) (10). How p18 imposes the requirement for v-cyclin in reactivation remains unclear and could involve either p18 action in virally infected cells or p18-dependent coordination of cell fate and function in noninfected cells. Using the β-lactamase-marked viral backbone, we utilized BAC recombination to regenerate a well-characterized cyclin-deficient γHV68 virus (cycKO). We further generated two recombinant viruses in which the v-cyclin gene was replaced by insertion of the cellular p18 gene (p18KI) tagged with a 3×FLAG epitope tag under viral control of the v-cyclin promoter and 3′ untranslated region (UTR) (10) (Fig. 1A). One of the p18KI viruses was generated on the β-lactamase-marked virus backbone (p18KI.βla), while the other was generated on the conventional, unmarked virus backbone (p18KI). These p18KI viruses lack expression of the viral cyclin and instead express p18 under the same viral transcriptional control as that of v-cyclin within infected cells. (Fig. 1A). The p18KI viruses give us the ability to interrogate the role of p18 expression specifically within infected cells.

To analyze v-cyclin and p18 expression, 3T12 fibroblasts were lytically infected with either the WT.βla, cycKO.βla, p18KI.βla, or p18KI virus. Analysis of these infected cell lysates demonstrated that, as expected, the cycKO.βla and both p18KI viruses express no v-cyclin, and that only lysates from cells infected with the p18KI viruses show detectible p18 (Fig. 1B).

Previous work showed that addition of β-lactamase to the wild-type virus does not alter the growth and replication of these viruses (19, 20). To compare virus replication of cycKO.βla, p18KI.βla, and p18KI, we infected 3T12 cells for a multistep replication analysis to measure production of infectious virus. While there were subtle yet statistically significant differences between WT.βla and cycKO.βla virus and between WT.βla and p18KI.βla virus at some time points, replication analysis revealed no dramatic differences in virus replication and production among these viruses (Fig. 1C).

To determine whether these viruses were equivalent in their capacity to report infection by β-lactamase activity, we assessed β-lactamase expression in lytically infected 3T12 cells with unmarked γHV68 (WT), WT.βla, cycKO.βla, or p18KI.βla virus. After 24 h, cells were harvested and stained for β-lactamase using the fluorescent cell-permeable β-lactamase substrate CCF2-AM. Uptake of the substrate causes the cells to fluoresce at 520 nM, and upon β-lactamase cleavage, the fluorescence shifts to 448 nM. Flow-cytometric analysis showed that lytic infection with WT.βla, cycKO.βla, and p18KI.βla viruses all resulted in an equivalent frequency of infected and β-lactamase-expressing cells, demonstrating that the β-lactamase marking system functions equivalently in each virus (Fig. 1D).

p18 inhibits γHV68 reactivation in a cell-intrinsic manner. Previously we determined that the reactivation defect of the cycKO virus was dependent on expression of p18 by the host; therefore, we generated the p18KI viruses to analyze whether

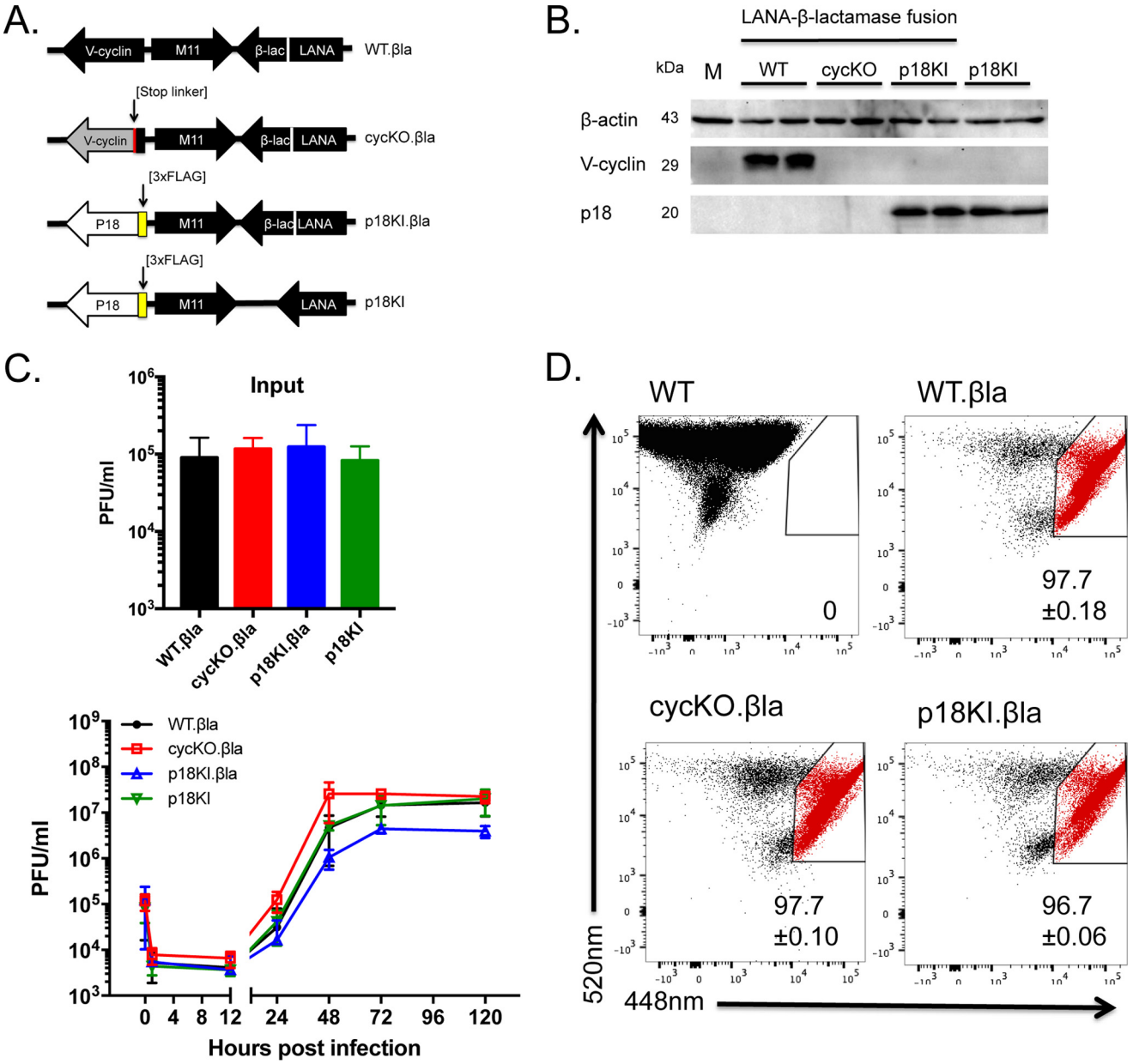

FIG 1 Generation and validation of β-lactamase-marked cyclin knockout and p18 knock-in viruses. (A) Schematic of β-lactamase-marked viruses and unmarked p18KI virus. The region of γHV68 from genome coordinates 102426 to 104868 is depicted to highlight mutated features in LANA and v-cyclin viral genes. Names of recombinant viruses are shown on the right. The stop codon for the cycKO.βla virus is indicated as a red bar, while 3xFLAG epitope tags are indicated as yellow bars. (B) Western blot of p18 and v-cyclin expression. 3T12 cells were infected with the indicated viruses at an MOI of 10 or mock infected (M) and cultivated for 24 h, and then protein was collected for immunoblot analysis of p18, v-cyclin, and loading control β-actin. Immunoblot antibodies and molecular masses are indicated on the left. Blot shown is representative of two independent experiments. (C) Multistep replication analysis of β-lactamase-marked WT, cycKO, and p18KI viruses. 3T12 cells were infected with the indicated viruses (MOI of 0.05). (Top) Titers of input virus were determined, with no significant differences identified. (Bottom) Infected cells and supernatants were harvested at the indicated times, and viral replication was measured by plaque analysis. Four independent replication analyses were completed with at least 3 technical replicates per sample ($n = 4$). Error bars shown represent the standard errors of the means (SEM). Unpaired *t* tests were performed at each time point among viruses, with statistically significant differences found between the cycKO.βla and WT.βla viruses at 12, 24, 48, and 72 h and between p18KI.βla and WT.βla viruses at 48, 72, 96, and 120 h. (D) Identification of infected cells through flow-cytometric analysis of β-lactamase activity. 3T12 cells were infected as described for panel B, collected at 24 h, and stained for β-lactamase activity. βla^+ cells are located in the upper right polygon and are shaded red. Numbers indicate the average percentage of βla^+ cells ± SEM ($n = 3$). Cells were previously gated on forward scatter and side scatter and doublet discrimination to identify single cells. Representative dot plots are shown.

regulation of reactivation was systemic or cell intrinsic (15). To limit p18 expression exclusively to infected cells, we inoculated $p18^{-/-}$ mice via intraperitoneal (i.p.) injection with 1×10^6 PFU/mouse of WT.βla, cycKO.βla, or p18KI.βla virus. i.p. infection results in a consistent maximal cycKO defect in reactivation measured in the peritoneal

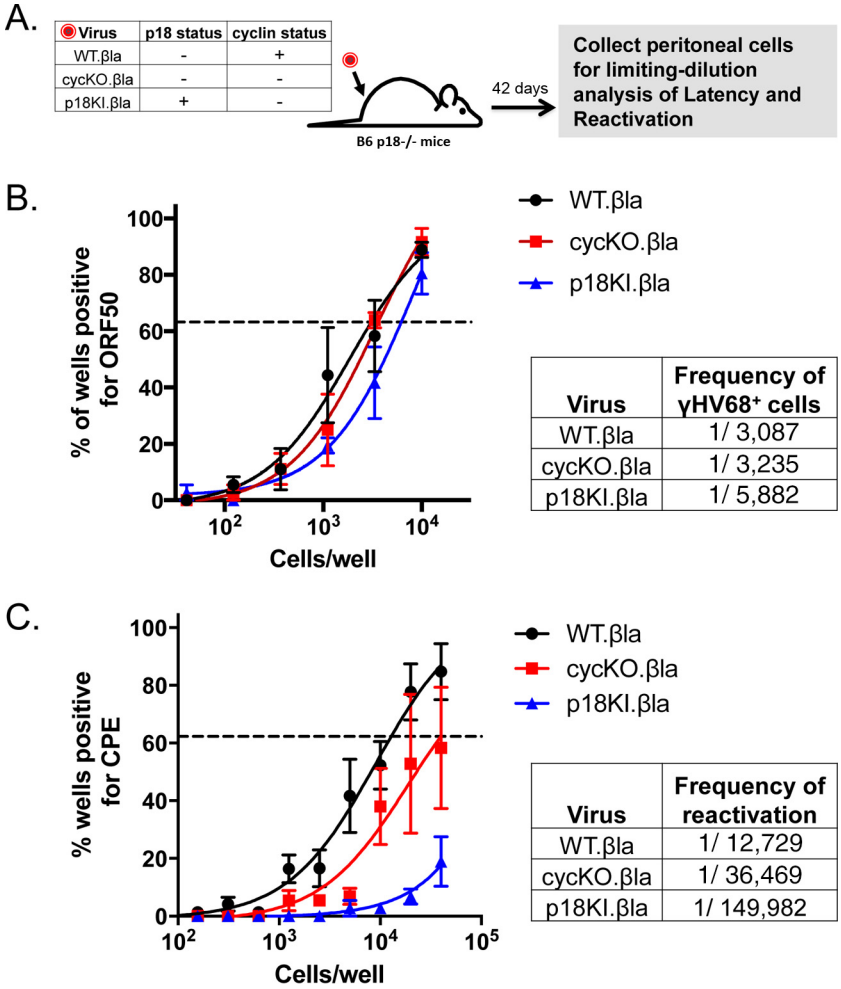

FIG 2 p18 expression inhibits viral reactivation in a cell-intrinsic manner in p18$^{-/-}$ mice. (A) Schematic of experimental timeline, denoting presence or absence of host p18 and viral cyclin in the recombinant viruses. p18$^{-/-}$ mice were inoculated with 1×10^6 PFU via i.p. injection with WT.βla (black), cycKO.βla (red), or p18KI.βla (blue) virus. At 42 dpi, peritoneal cells were harvested and plated in limiting-diluting fashion for either PCR analysis for the presence of the viral genome (B) or reactivation analysis (C). The frequency of latently infected or reactivating cells was determined by Poisson distribution, where the number of cells per well corresponding to 63.2% (dotted line) is the frequency at which at least one cell is harboring viral genome (B) or reactivating virus (C) ($n = 3$, with 4 to 5 mice per experiment). Error bars represent SEM. Nonlinear regression analysis showed a statistical difference between the number of WT.βla versus p18KI.βla latently infected cells (*, $P = 0.04$) and cycKO.βla versus p18KI.βla latently infected cells (*, $P = 0.008$) but not WT.βla versus cycKO.βla latently infected cells. Nonlinear regression analysis also showed a statistical difference between the number of WT.βla versus cycKO.βla reactivating cells (*, $P = 0.0003$). Comparisons with the p18KI.βla virus could not be made as the curve never reached 63.2, showing an extreme defect in reactivation.

cells and provides direct seeding of latent tissue reservoirs. After 42 days postinfection (dpi), a time when long-term latency is stably established and preformed virus from the primary infection has been cleared, peritoneal cells were collected. First, to test whether establishment from latency is altered, we performed a limiting-dilution nested PCR analysis for viral gene ORF50 DNA. This analysis showed that infection with the WT.βla and cycKO.βla viruses resulted in an equivalent frequency of latently infected cells, with a 0.55-fold decrease in the frequency of cells latently infected with the p18KI.βla virus (Fig. 2B). One of 3,087 cells was latently infected with WT.βla virus, one of 3,235 cells with cycKO.βla virus, and one of 5,882 cells with p18KI.βla virus (Fig. 2B). We next measured reactivation from latency, using an *ex vivo* limiting-dilution reactivation assay on permissive murine embryonic fibroblast (MEF) monolayers. Peritoneal cells from p18$^{-/-}$ infected mice were plated on permissive MEF monolayers for analysis of

cytopathic effect (13, 21). This analysis showed that the cycKO.βla virus reactivated at a frequency nearly equivalent (0.35-fold) to that of WT.βla in p18-deficient cells, as previously observed using unmarked versions of these viruses (Fig. 2C) (15). At least one of every 12,729 peritoneal cells plated contained a cell-reactivating WT.βla virus, and at least one of 36,469 cells contained reactivating cycKO.βla virus (Fig. 2C). In contrast, cells latently infected with the p18KI.βla virus showed a severe defect in reactivation from latency compared to either WT.βla or cycKO.βla: one of every 149,982 cells contained a reactivating p18KI.βla virus (Fig. 2C). When p18 is expressed from the p18KI.βla virus in $p18^{-/-}$ cells, a process that occurs exclusively in infected cells, there is a profound defect in reactivation, similar to what is observed following infection of normal ($p18^{+/+}$) B6 mice with cycKO virus (10). These data demonstrate that p18 expression only within latently infected cells is sufficient to restrict reactivation and therefore acts in a cell-intrinsic manner.

Infected cell compositions are not altered between WT.βla, cycKO.βla, and p18KI.βla viruses. Based on the observation that p18 expression inhibits reactivation in a cell-intrinsic manner, we tested whether the p18KI virus had an altered cellular distribution that could contribute to the defect in p18KI.βla virus reactivation in $p18^{-/-}$ mice. We infected $p18^{-/-}$ mice, collected peritoneal cells at 42 dpi, and then treated cells with the β-lactamase substrate and stained with conventional flow antibodies to surface proteins (19). Consistent with our previous limiting-dilution PCR analysis, there was no difference between the frequencies of total $LANA^+$ (βla^+) cells between the WT.βla-, cycKO.βla-, and p18KI.βla-infected mice (Fig. 3A). Cell types known to support latent infection include multiple subsets of B cells, macrophages, and dendritic cells (2, 22–25). Although B cells are thought to be the primary cell type responsible for splenic reactivation, it has been proposed that in the peritoneum, macrophages and B1 cells (a subset of B cells consisting of B1-a and B1-b cells) are the main pool of reactivating cells (23, 26). It is possible that although the total numbers of latently infected cells are similar between these viruses, the composition of p18KI.βla-infected cells might be skewed toward a different cell subtype which is less permissive to reactivation from latency. To address this possibility, cells were treated with the β-lactamase substrate CCF2-AM and stained with CD19, B220, and CD5 antibodies to identify B cells and B cell subsets. The composition of infected peritoneal B cells was analyzed first by CD19 expression to identify total B cells ($CD19^+$) versus non-B cells ($CD19^-$) (Fig. 3B) and separately analyzed to identify B cell subsets, including B2 cells ($B220^{high}/CD5^-$), B1-a cells ($B220^+/CD5^+$), and B1-b cells ($B220^{int}/CD5^-$) (Fig. 3C). The distribution of infected cells was skewed toward B cell infection in viruses lacking v-cyclin (cycKO.βla and p18KI.βla). Although the difference was not statistically significant, ~20% more of the cycKO.βla- and p18KI.βla-infected cells were $CD19^+$ than the WT.βla-infected cells. Within the limitations of a few infected cells, there were no significant differences among B cell subsets in the infected cell compositions between the cycKO.βla- and p18KI.βla-infected cells (Fig. 3C). The peritoneal B cell subset composition of the viruses was approximately 20 to 30% conventional B2 cells, 15 to 20% B1-a cells, and 15 to 30% B1-b cells. From these data, we conclude that the lack of v-cyclin results in a greater percentage of infected B cells with both the cycKO.βla and p18KI.βla viruses, yet relative to the cycKO virus, the p18KI.βla virus results in a more severe reactivation defect. The decreased reactivation frequency of the p18KI virus does not correspond to alterations in the frequency or composition of infected cells.

p18 expression attenuates progression of acute pneumonia. v-cyclin plays a critical role in multiple aspects of γHV68 pathogenesis, ranging from acute to chronic pathologies (27–29). We next reasoned that because a primary function of the v-cyclin is to overcome a cell-intrinsic p18 barrier, the p18KI virus might show additional disease attenuation beyond that observed during cycKO infection. We previously described an acute disease model of highly inflammatory viral pneumonia, instigated by γHV68 infection, that has been used to measure pathogenesis of a number of γHV68 mutant viruses (20, 27, 30, 31). In this model, intranasal (i.n.) γHV68 inoculation of BALB/c

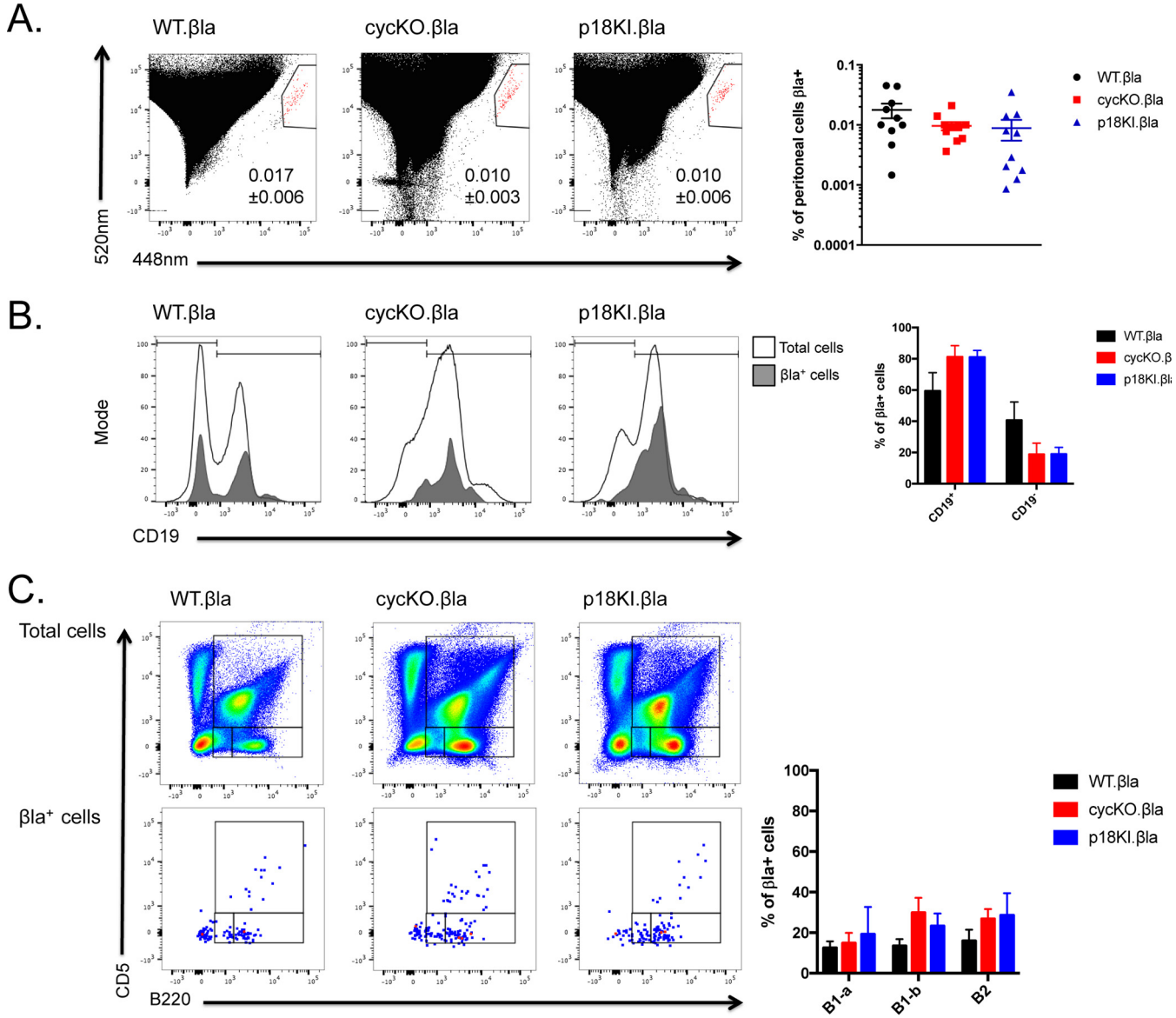

FIG 3 p18 expression does not alter composition of infected B cells. p18$^{-/-}$ mice were infected with the WT or with cycKO- or p18KI-marked virus. At 42 dpi, peritoneal cells were isolated and stained for β-lactamase activity, identifying infected cells through LANA expression. (A) Representative dot plots are shown, with average percentages of βla$^+$ cells ± SEM indicated below. The scatter plot on the right indicates the percentage of βla$^+$ cells for each mouse. Unpaired *t* tests were used to compare the percentage of βla$^+$ cells between each virus, with no significant difference found ($n = 10$). (B and C) Infected peritoneal cell composition was analyzed by flow-cytometric analysis of cell surface markers on β-lactamase-positive cells. (B) Peritoneal B cells and non-B cells were distinguished by CD19 expression. Representative histogram overlays of CD19 expression are shown for WT.βla-, cycKO.βla-, and p18KI.βla-infected mice on the left. CD19 expression on total cells is indicated by the unfilled, black trace. CD19 expression on βla$^+$ cells is indicated by the shaded histogram. The bar graph on the right indicates the average percentage (±SEM) of βla$^+$ cells that are CD19$^+$ or CD19$^-$ ($n = 6$). Unpaired *t* tests and one-way ANOVA revealed no statistically significant differences between viruses. (C) Peritoneal B cell subsets were defined by expression of B220 and CD5, with B1-a cells being B220$^+$ CD5$^+$, B1-b cells being B220^{int} CD5$^-$, and conventional B2 cells being B220^{hi} CD5$^-$. Representative pseudocolor plots are shown with the total cell populations shown at the top and βla$^+$ gated populations shown at the bottom. The bar graph on the right indicates the percentage of βla$^+$ cells that were B1-a, B1-b, or B2 cells ± SEM. Unpaired *t* tests were used to measure differences between the viruses for the percentage of B1-a, B1-b, and B2 cells in the βla$^+$ cells with no significant differences found among the B cell subsets ($n = 6$).

gamma interferon-deficient (IFN-γ$^{-/-}$) mice results in lethal viral pneumonia over the course of 15 days. IFN-γ has previously been shown to be a significant regulator of virus infection. IFN-γ represses viral infection and reactivation from latency such that mice that are either deficient in the cytokine (IFN-γ$^{-/-}$) or are nonresponsive to IFN-γ (IFN-γR$^{-/-}$) are susceptible to γHV68-induced pathologies (32, 33). Given that these mice are defective in controlling infection and associated disease, this model provides a highly useful screen of pathogenesis. We previously showed that 4 × 10^5 PFU of

wild-type virus is lethal in ~40 to 60% of the mice infected, while the same dose of cycKO virus results in development of pneumonia, as demonstrated by lung histology at 8 dpi, but no disease signs or morbidity, demonstrating that the reactivation-defective cycKO virus results in attenuated pathogenesis (27). The p18KI virus is both cyclin deficient and expresses exogenous p18 within infected cells, is further attenuated in reactivation relative to the cycKO virus, and therefore could be further attenuated in disease relative to the cycKO virus. However, because the cycKO virus does not cause lethal pneumonia at the standard dose, we tested if a higher inoculation dose could confer virulence in the cycKO.βla-infected mice. We intranasally inoculated IFN-$\gamma^{-/-}$ mice with either 4×10^5 PFU/mouse of WT, 4×10^5 PFU/mouse of cycKO, or 4×10^7 PFU/mouse (100×) of cycKO virus. Over the course of 15 days, mice were scored on development of disease signs and were euthanized if moribund. As previously reported, inoculation with the standard 4×10^5 PFU of cycKO virus resulted in no lethal pneumonia (0/3), whereas 40% (2/5) of the WT-infected mice succumbed to viral pneumonia. Inoculation of the mice with a 100× dose of cycKO virus indeed resulted in virulence, with 80% (4/5) of mice infected becoming moribund (Fig. 4A). These data show that increasing the initial titer of cycKO virus can overcome the cycKO defect in virulence and allow a window for comparison of pathogenesis with the p18KI virus.

Based on the virulence observed upon high-dose inoculation with cycKO virus, we examined if p18KI virulence was attenuated in relation to the cycKO virus. Given the severity of the disease in the mice infected with 100× cycKO virus (Fig. 4A), we chose to compare the cycKO and p18KI viruses at 50× standard doses to ensure that any attenuation of the p18KI virus relative to the cycKO virus could be detected. We inoculated BALB/c IFN-$\gamma^{-/-}$ mice with 4×10^5 PFU of WT or 2×10^7 PFU (a 50× dose) of cycKO or p18KI virus and analyzed disease progression over the course of 15 days. Inoculation with the 50× cycKO virus resulted in severe disease, with 65% (13/20) of infected mice becoming moribund, similar to the low-dose WT virus, which resulted in 78% (14/18) lethal pneumonia. The p18KI virus resulted in a far lower rate of lethal pneumonia than the cycKO virus, with only 30% (6/20) of the infected mice succumbing to viral pneumonia. Statistical analysis demonstrated differences between the WT virus compared with the p18KI virus and between the cycKO virus compared with the p18KI virus. Additionally, the p18KI virus resulted in a delayed lethal pneumonia compared to that of the other viruses (Fig. 4B).

To analyze the development of inflammation and acute pneumonia after infection with the p18KI virus, IFN-$\gamma^{-/-}$ mice were inoculated with WT, cycKO, or p18KI virus. These mice were euthanized at 7 dpi, a time point that corresponds to early disease signs after infection with the WT virus. The lungs from these mice were collected for histological analysis and quantification of virus by quantitative PCR (qPCR) for viral DNA. Hematoxylin and eosin (H&E) staining showed that at 7 dpi, all three viruses induced pneumonia. Lung tissue was scored based on extent and location of infiltration and indicated mild infiltration in WT (4×10^5 PFU) infection, moderate infiltration in p18KI infection (2×10^7 PFU), and severe infiltration in cycKO infection (2×10^7 PFU). All mice developed a high degree of edema associated with a heavy influx of neutrophils, as well as formation of perivascular lymphocytic infiltration (Fig. 4C). Despite the attenuation in lethality, the p18KI virus is not attenuated in initiation of inflammation and pneumonia.

Based on our previous temporal characterization of virus production, we measured virus DNA in infected lungs at 7 dpi, a time at which cyclin-deficient virus production is notably decreased relative to that of the WT and before terminal disease signs are generally noted (27). To measure the amount of virus present in the lungs, 7-dpi lung tissue was digested and DNA was extracted. Quantitative PCR for viral DNA was performed with primers directed to the glycoprotein B (gB) gene as an indication of the amount of virus present. Infection with the WT, cycKO, and p18KI viruses resulted in large amounts of viral DNA present in the lung at 7 dpi. While there was less virus present in the p18KI- and cycKO-infected lungs than in the wild type, there was no apparent difference between the cycKO and p18KI viruses (Fig. 4D). Therefore, these

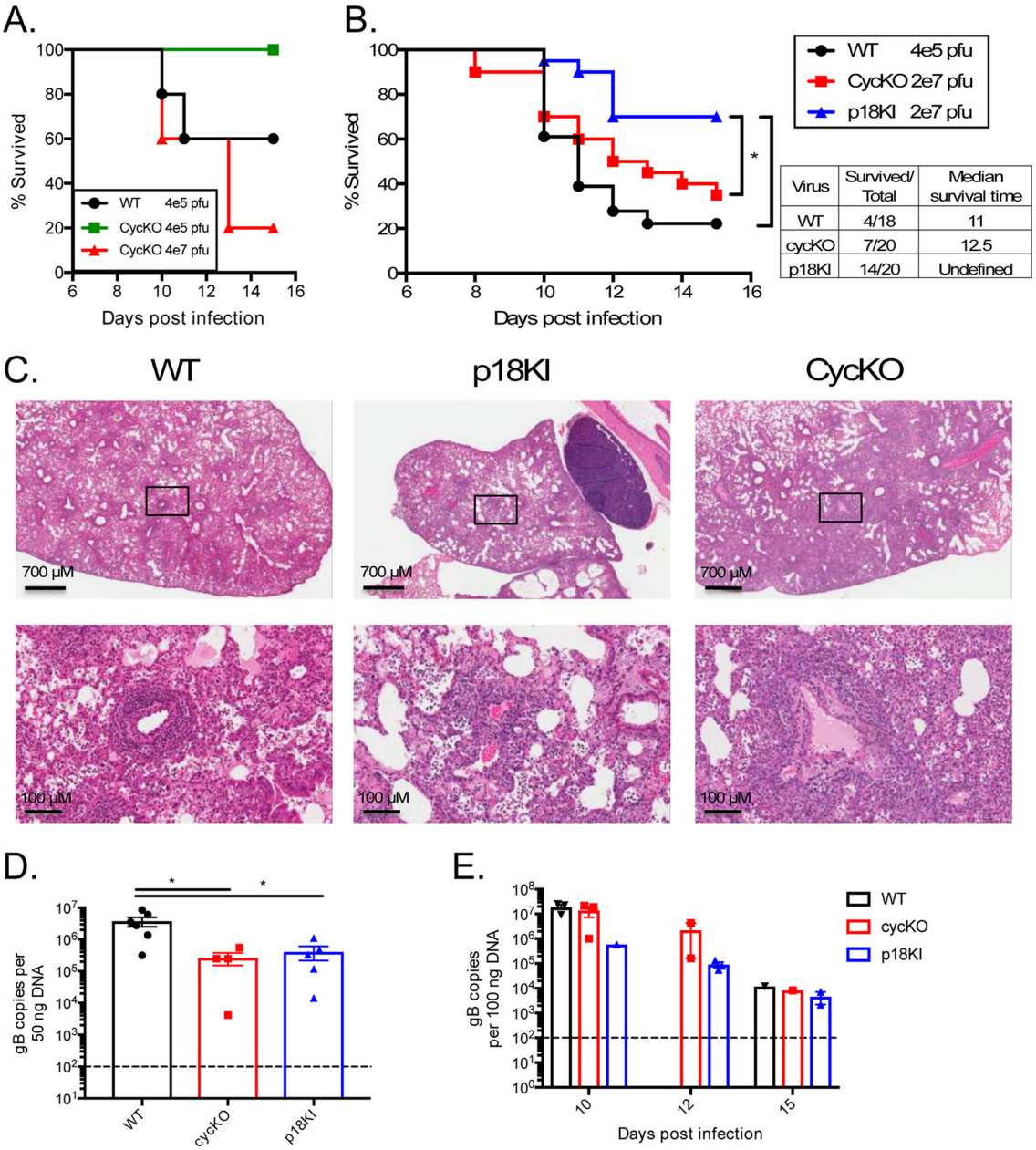

FIG 4 p18 expression attenuates progression of lethal pneumonia. (A) IFN-$\gamma^{-/-}$ mice were inoculated i.n. with WT (black) or cycKO (green) virus at 4×10^5 PFU/mouse or cycKO (red) virus at 4×10^7 PFU/mouse. Disease signs were scored and monitored for 15 dpi for development of viral pneumonia. Mice that reached a maximal lethargy score were considered moribund and euthanized. Any mice that did not succumb to pneumonia were euthanized at 15 days postinfection ($n = 5$ for WT virus, $n = 3$ for cycKO virus at 4×10^5 PFU, and $n = 5$ for cycKO virus at 4×10^7 PFU). (B) IFN-$\gamma^{-/-}$ mice were inoculated i.n. with WT (black) virus at 4×10^5 PFU/mouse, cycKO (red) virus at 2×10^7 PFU/mouse, or p18KI (blue) virus at 2×10^7 PFU/mouse. Disease and lethal pneumonia were measured as described for panel A. The graph shows survival from 4 independent experiments each with 3 to 5 mice ($n = 18$ for WT virus and $n = 20$ for cycKO and p18KI viruses). The Gehan-Breslow-Wilcoxon test was used to compare survival curves between WT and p18KI viruses (***, $P = 0.0008$) and cycKO and p18KI viruses (*, $P = 0.0212$), with no significant difference found between WT and cycKO viruses. Additionally, the log-rank (Mantel-Cox) test was performed for WT compared to p18KI (***, $P = 0.0009$) and cycKO compared to p18KI (*, $P = 0.0194$) viruses, and no significance was found between WT and cycKO viruses. (C and D) IFN-$\gamma^{-/-}$ mice were infected as described for panel B, with all mice euthanized at 7 dpi. Lung samples were fixed in 10% formalin–PBS, paraffin embedded, and stained with H&E, and infiltration was analyzed by histology at 40× (top) and 400× (bottom), with scale bars included in each image (C) or lysed to collect DNA prior to virus quantitation by qPCR for viral gB DNA (D). Viral gB DNA was quantified from 50 ng of lung DNA, and the total amount of gB DNA was calculated using a gB plasmid standard. Error bars represent SEM. One-way ANOVA with Tukey's multiple-comparison test was performed among viruses, and significance was found with adjusted P values comparing WT to p18KI virus (*, $P = 0.0447$) and WT to cycKO virus (*, $P = 0.0403$) ($n = 6$ for WT, $n = 4$ for cycKO, and $n = 5$ for p18KI). (E) Lung tissue was collected from moribund mice depicted in panel B at the indicated days postinfection. DNA was isolated and viral gB levels were quantitated using qPCR from 100 ng of lung DNA. At 10 dpi, $n = 3$ for WT, $n = 3$ for cycKO, and $n = 1$ for p18KI; at 12 dpi, $n = 2$ for cycKO and $n = 3$ for p18KI; at 15 dpi, $n = 1$ for WT, $n = 1$ for cycKO, and $n = 2$ for p18KI.

data suggest that the decreased lethal pneumonia of the p18KI virus relative to the cycKO virus is not due to an early defect in development of inflammation and pneumonia or in the amount of virus in the lungs but rather a difference in progression versus resolution of pulmonary inflammation and pneumonia. To test whether virus production and resolution differs among these viruses at later time points, viral DNA from tissues of mice euthanized for lethal pneumonia was quantified (Fig. 4E). Comparison of viral DNA from these lungs suggests that despite virus production equal to that of cycKO virus at 7 dpi, p18KI virus is decreased relative to cycKO at late times postinfection, corresponding to attenuation of disease progression. These data demonstrate that in the context of acute viral pneumonia, a v-cyclin-dependent pathology, expression of p18 is sufficient to enhance virus attenuation even in p18-sufficient hosts.

DISCUSSION

Reactivation from latency is a critical hub for the γHV life cycle and the induction of virus-associated pathologies. A comprehensive understanding of the drivers and repressors of reactivation is important for effectively targeting different stages of γHV infection and treating disease. Previous work has identified numerous viral and host genes that regulate γHV reactivation through different means. γHV68 and KSHV encode a suite of latency-associated genes, including LANA and v-cyclin genes. LANA supports the maintenance of latency by suppressing lytic gene expression, inhibiting lytic replication, and maintaining the latent viral genome (34–36). v-cyclin has been well established as a viral protein required for reactivation from latency (10, 13). Virus lacking the viral cyclin is severely attenuated in reactivation from latency despite successful establishment of latency.

Despite the clear role of v-cyclin in reactivation, little is understood in how v-cyclin performs its function. Being a homologue of host D-type cyclins suggests that v-cyclin promotes reactivation through conventional cyclin/cell cycle actions. While v-cyclin is able to bind and activate CDKs to promote cell cycle progression, reactivation appears to be independent of this, since a v-cyclin variant containing point mutations abrogating interaction with CDKs is still able to promote reactivation (37, 38). Additionally, using a panel of recombinant γHV expressing host cyclins in place of the viral cyclin, reactivation was complemented by only the host cyclin D3 and not other host cyclins (14). Given that other host cyclins are stronger activators of kinase activation and cell cycle progression, cell cycle progression may not necessarily be the mechanism of reactivation. One recently discovered role of v-cyclin in reactivation from latency is its apparent antagonism of host $p18^{INK4c}$ (15). Here, by using p18 expressing γHVs, we demonstrated that cell-intrinsic host p18 imposes a requirement for viral cyclin in optimal infection and pathogenesis of γHV68. Over the years, several studies have uncovered novel roles for host CDKs, cyclins, and cyclin kinase inhibitors, such as p18, unrelated to cell cycle regulation or proliferation (39). Thus, it remains possible that v-cyclin and p18 regulate reactivation through non-cell cycle mechanisms, such as regulating host and/or viral gene expression, and, in turn, regulating reactivation.

As mentioned above, reactivation from latency has a strong association with numerous γHV-associated disease outcomes. In this study, we utilized a model of acute lethal pneumonia in reactivation-prone mice to determine whether p18 repression of reactivation corresponded to attenuated disease. We found that exogenous p18 expression from the p18KI virus resulted in a large reduction in lethality in this model. This reduced lethality was not associated with a failure to induce large amounts of inflammation or virus present in the lung. This suggests instead that infection with the p18KI virus is associated with better resolution of pneumonia. Although it is not completely clear what skews the lung toward resolution of pneumonia and clearance after infection with the p18KI virus, it is possible that this is a result of lytic replication, with further diminution of reactivation compared to the cycKO virus or with a combination of those factors with tissue resolution. In previous work, we have shown that the cycKO virus has reduced viral titers relative to those of WT infection in this model. Compared to WT virus, depressed titers are observed as early as 5 days postinfection, resulting in

clearance of virus and return to lung homeostasis (27). As the cycKO virus does not have a replication defect *in vitro*, failure to maintain high titer likely is due to insufficient reactivation once virus has entered latency. In this report, we show that increasing the inoculating dose of virus 50-fold circumvents this defect and allows the cycKO virus to maintain high levels of virus (Fig. 4D). Although the cycKO virus is severely defective in reactivation from latency, low levels of reactivation still occur, presumably through host cyclins. p18 expression from the p18KI virus likely is able to inhibit this low level of reactivation even further, as host cyclins are highly susceptible to inhibition by CDKIs such as p18.

This work shows p18 having therapeutic potential in virus-associated disease outcomes. Future directions include testing whether host p18 expression can reduce the incidence of other v-cyclin-dependent γHV-associated diseases, such as lymphoproliferative disorders and development of malignancies. Manipulation of p18 may provide a new avenue of host modulation to alter virus infection (15, 40–42). While our current studies have focused on γHV68, it is notable that there is evidence for roles of p18 in the human γHVs. For example, proteomic analysis demonstrates KSHV v-cyclin interaction with p18 (17). EBV-associated Hodgkin's disease is associated with decreased or lack of p18 expression, and recent work from the Allday group demonstrates a strong correlation of p18 expression with EBV transformation (43, 44). It would also be of value to determine if p18 is beneficial in recovery from other, non-γHV, viral infections, such as herpes simplex virus and cytomegalovirus. Ultimately, defining how p18 molecularly imposes the requirement for v-cyclin in reactivation will be a critical question to address, a question that now can be interrogated through (i) mutational analysis of p18 using this platform combined with (ii) purification of latently infected cells using the β-lactamase marking system, followed by detailed molecular analysis.

MATERIALS AND METHODS

Cell lines. 3T12 mouse fibroblast cells (ATCC CCL-164) were cultured in 5% fetal bovine serum–Dulbecco's modified Eagle's medium (FBS-DMEM) with 20 U of penicillin and 20 μg of streptomycin per ml and 4 mM L-glutamine. Mouse embryonic fibroblasts (MEFs) were isolated as described and cultured in 10% FBS–DMEM with 20 U of penicillin, 20 μg of streptomycin per ml, 4 mM L-glutamine, and amphotericin B (Fungizone) at 250 ng/ml (45).

Viruses. The β-lactamase-marked cycKO virus was generated by BAC recombination (46). The original cycKO virus and wild-type β-lactamase virus backbones were utilized in generation of this cycKO.βla (10, 19). A translational stop cassette was inserted into the ORF72 gene by BAC recombination. PCR was performed with the mutagenic primers containing the stop point mutation (forward, 5′-GTT ATC CTG ACG GAG GTC TTT GCA CAC ACA AAA CAT CCA CGG CTA GTT AAC TAG CCG TGG TTA GGA CTT TCC TGT ATC GAT TTA TTC AAC AAA GCC ACG-3′; reverse, 5′-ACC AGC ACT TTA CTT CCC AAT ACA GGA AAG TCC TAA CCA CGG CTA GTT AAC TAG CCG TGG ATG TTT TGT GTG TGC ACG CGT ATA TCT GGC CCG TAC ATC G-3′) along with the pEP-KanS plasmid template. The PCR product containing the Kan/I-SceI insert was DpnI treated, run on a 1% Tris-acetate-EDTA (TAE)-agarose gel, and gel purified. This product was electroporated into recombinant/electrocompetent GS1783 cells containing either the original WT BAC DNA or the β-lactamase-marked WT BAC DNA. Proper recombination was checked by chloramphenicol and kanamycin selection along with digestion of the recombinant BAC compared to WT BAC DNA digested with HindIII and BglII. Resolution of the cointegrates was performed by inducing the I-SceI enzyme with 1% L-arabinose. Screening of the second recombination was done by PCR confirmation and by restriction digest with HindIII and HpaI. BAC DNA that passed this screening was transfected into Vero-Cre cells to remove the LoxP-flanked BAC sequence from the viral genome.

Similarly, the p18 knock-in viruses were generated by BAC recombination in which the cDNA expression cassette for mouse p18^{INK4c} was inserted in place of the viral cyclin. The p18 expression cassette was placed under the control of the viral cyclin promoter and 3′ UTR. Briefly, in order to create the targeting construct for BAC recombineering, two separate gBLOCKS (IDT) were assembled using Gibson Assembly (NEB). This fragment was PCR amplified, purified from the gel, and used for a second round of Gibson assembly using PCR-amplified flanking regions (to facilitate recombination into the BAC). The entire targeting construct was PCR amplified, gel purified, and electroporated into *Escherichia coli* strain GS1783 harboring either an original WT BAC or a β-lactamase-marked WT BAC. Chloramphenicol- and kanamycin-resistant colonies were screened by PCR for correct insertions and then were subjected to a resolution step to remove the kanamycin resistance cassette and create the desired genetic modifications (46). The resulting BAC β-lactamase-marked cycKO and p18 knock-in viruses were partially sequenced (Laragen, Culver City, CA, USA) to ensure the desired sequences were present. Lastly, the BACs were screened by restriction fragment length polymorphism (RFLP; using HindIII, EcoRI, and BamHI) to ensure BAC integrity prior to transfection. New recombinant virus BACs were transfected into 293 cells to generate BAC-containing virus. BAC virus then was used to infect Vero-Cre cells (a kind gift of David Leib) for selection and removal of BAC DNA from virus (47, 48). The viruses resulting from these processes

were the β-lactamase-marked cyclin-deficient γHV68 (cycKO.βla), the β-lactamase-marked p18 knock-in virus expressing p18 in place of the viral cyclin (p18KI.βla), and the unmarked p18 knock-in γHV68 virus expressing p18 in place of the viral cyclin (p18KI).

Mice. $p18^{INK4c-/-}$ mice ($p18^{-/-}$) on a C57BL/6 background were previously described (49). BALB/c interferon gamma-deficient mice (IFN-$\gamma^{-/-}$) were originally obtained from Jackson Laboratory [strain C.129S7(Bg)-Ifngtm1Ts/J; stock no. 002286]. All mice were bred in-house at the University of Colorado Denver Anschutz Medical Campus in accordance with university regulations and the Institutional Animal Care and Use Committee.

Immunoblotting. 3T12 cells were infected at a multiplicity of infection (MOI) of 10 and incubated for 24 h. Cells were lysed in radioimmunoprecipitation assay (RIPA) buffer (containing 1 mM dithiothreitol, 1 μg/ml aprotinin, 1 μg/ml leupeptin, 50 μg/ml phenylmethylsulfonyl fluoride), and 80 μg of protein was resolved by 12% SDS-PAGE and transferred to a polyvinylidene difluoride membrane at 10 V for 1.25 h. Blots were incubated overnight in primary antibody at 4°C with rocking, washed, and incubated with secondary antibody using the Millipore SNAP i.d. 2.0 system. Briefly, wash buffer consisted of 0.05% Tween 20 in phosphate-buffered saline (PBS), and incubation with secondary antibody was at 1:2,000 for 10 min at room temperature. Primary antibodies were diluted in 2.5% nonfat milk in 0.05% Tween 20–PBS. Primary antibody consisted of 1:20,000 β-actin (A5316; Sigma-Aldrich), 1:1,000 p18 (sc-865; Santa Cruz), and 1:500 v-cyclin (10). Secondary antibodies were diluted in 0.5% nonfat milk in 0.05% Tween 20–PBS. Secondary antibodies were 1:2,000 donkey anti-mouse horseradish peroxidase (HRP) (715-035-151; Jackson Laboratories) or 1:2,000 donkey anti-rabbit HRP (NA9340; GE Healthcare). Signal was detected using ECL Prime Western blotting solution (RPN2232; GE Healthcare). Blots were stripped using ReBlot Plus strong antibody stripping solution (2504; Millipore) between probings.

Multistep replication analysis. 3T12 cells were infected with either WT.βla, cycKO.βla, p18KI.βla, or p18KI virus at an MOI of 0.05 PFU/cell. Total cells and supernatant were collected at various times postinfection and frozen at −80°C (including input virus) for titer analysis. Cells and supernatants were frozen and thawed three times to disrupt cells prior to serial dilution into 5% FBS–DMEM (with amphotericin B; 250 ng/ml) for plaque quantification and calculation of virus titer based on plaque standards (10). Titers of input virus were determined the same way but without three rounds of freezing and thawing.

Flow cytometry analysis. Peritoneal cells were collected with 10 ml of cold 1% FBS–DMEM. β-Lactamase activity was detected using the LiveBLAzer FRET-BG/loading kit with CCF2-AM (K1025; Thermo Fischer Scientific) as previously described (19, 20, 22). Cell surface antibodies used were CD19 clone eBio1D3 Alexa Fluor 700 (56-0193-81; eBioscience), B220 clone RA3-6B2 allophycocyanin (APC; 17-0452-81; eBioscience) or APC-eFluor780 (47-0452-80; eBioscience), and CD5 clone 53-7.3 APC (17-0051-81; eBioscience) or APC-eFluor780 (47-0051-82; eBioscience). Fc blocking antibody 24g2 was used in staining to prevent any labeling of the Fc receptor.

Limiting-dilution analyses. Briefly, mice were inoculated with either WT.βla, cycKO.βla, or p18KI.βla virus at 1×10^6 PFU/mouse via intraperitoneal injection. After 42 days, peritoneal cells were collected and limiting-dilution plated for reactivation or PCR analysis. By Poisson distribution, the number of cells plated corresponding to 63.2% of the wells positive is the frequency at which there is at least one reactivating or genome-positive cell.

Reactivation analysis. Cell dilutions were plated on highly permissive MEF monolayers for quantification of wells demonstrating cell lysis as previously described (13, 23). To control for any preformed virus, mechanically disrupted peritoneal cells were plated in parallel; no monolayer disruption was observed in disrupted cells.

PCR analysis. Cell dilutions were subjected to in-plate DNA isolation and nested PCR for single-copy sensitivity detection of viral gene 50 DNA, with plasmid sensitivity controls included on each plate as previously described (13, 23).

Acute viral pneumonia. Lung pathology was analyzed as previously described (27). BALB/c IFN-$\gamma^{-/-}$ mice were infected via intranasal (i.n.) inoculation with the indicated doses of WT, cycKO, or p18KI virus. Disease signs were scored on a range of 0 to 3, with 3 being severe, and included ruffling, hunching, dehydration, conjunctivitis, and lethargy. Mice with a lethargy score of 3 were determined to be moribund and were euthanized. Mice surviving to 15 days were euthanized at termination of the experiment.

Quantitative real-time PCR. DNA was isolated from infected lungs of BALB/c IFN-$\gamma^{-/-}$ mice at 7, 10, 12, or 15 days postinfection (dpi) using the DNeasy blood and tissue kit (69506; Qiagen). Lung DNA was normalized to a concentration of 10 ng/μl (7 dpi) or 20 ng/μl (10, 12, and 15 dpi) for qPCR analysis of 50 ng or 100 ng of sample DNA using a LightCycler 480 probe kit (04707494001; Roche). The primers used for viral gB were the following: forward, GGCCCAAATTCAATTTGCCT; reverse, CCCTGGACAACTCCT CAAGC (50–52). gB plasmid standard dilution ranged from 10^{10} to 10^2 copies, with a limit of detection of 100 copies (52). Each lung sample was run as a technical triplicate.

Histology. Lung tissue collected from interferon gamma-deficient BALB/c mice at 7 dpi and from mice euthanized due to lethal pneumonia signs was stored in 10% formalin in PBS that was exchanged for fresh formalin after at least 24 h. Samples were processed by the University of Colorado Cancer Center Research Histology Shared Resource for paraffin embedding, sectioning, and staining with hematoxylin and eosin (H&E). All slides were analyzed in a blinded manner by a board-certified pathologist, Carlyne Cool. The infiltrates were scored on a quantitative scale of 0 to 3 (0, no infiltrate; 1, mild infiltrate; 2, moderate infiltrate; 3, severe infiltrate). The location of the infiltrates was assessed (i.e., peri-airway, perivascular, and parenchymal) and the subtype of inflammatory infiltrate determined (neutrophils, lymphocytes, and histiocytes). Additional features, such as interstitial or airspace edema, fibrin exudates,

necrosis, and reactive epithelial changes, were also assessed. Photographs were taken to demonstrate infiltrated tissue representative for each virus.

Statistical analysis and software. Flow-cytometric analysis was performed using FlowJo V.10.0.8r1. Graphs were generated and statistical analyses were performed using GraphPad Prism 7.0a. Limiting-dilution curves were created by performing a nonlinear regression, using log (agonist) versus response Find EC anything. F was set to 63.2, while the top and bottom of the curves were constrained to 100 and 0, respectively. Comparisons of the log ECF values were used to determine statistical significance. Unpaired Student *t* tests were performed as mentioned. One-way analyses of variance (ANOVA) were performed with Tukey's multiple-comparison test to find adjusted *P* values.

REFERENCES

1. Virgin HW, Latreille P, Wamsley P, Hallsworth K, Weck KE, Dal Canto AJ, Speck SH. 1997. Complete sequence and genomic analysis of murine gammaherpesvirus 68. J Virol 71:5894–5904.
2. Barton E, Mandal P, Speck SH. 2011. Pathogenesis and host control of gammaherpesviruses: lessons from the mouse. Annu Rev Immunol 29:351–397. https://doi.org/10.1146/annurev-immunol-072710-081639.
3. Speck SH, Ganem D. 2010. Viral latency and its regulation: lessons from the gamma-herpesviruses. Cell Host Microbe 8:100–115. https://doi.org/10.1016/j.chom.2010.06.014.
4. van Esser JW, van der Holt B, Meijer E, Niesters HG, Trenschel R, Thijsen SF, van Loon AM, Frassoni F, Bacigalupo A, Schaefer UW, Osterhaus AD, Gratama JW, Löwenberg B, Verdonck LF, Cornelissen JJ. 2001. Epstein-Barr virus (EBV) reactivation is a frequent event after allogeneic stem cell transplantation (SCT) and quantitatively predicts EBV-lymphoproliferative disease following T-cell-depleted SCT. Blood 98:972–978. https://doi.org/10.1182/blood.V98.4.972.
5. Cesarman E, Nador RG, Bai F, Bohenzky RA, Russo JJ, Moore PS, Chang Y, Knowles DM. 1996. Kaposi's sarcoma-associated herpesvirus contains G protein-coupled receptor and cyclin D homologs which are expressed in Kaposi's sarcoma and malignant lymphoma. J Virol 70:8218–8223.
6. Chang J, Renne R, Dittmer D, Ganem D. 2000. Inflammatory cytokines and the reactivation of Kaposi's sarcoma-associated herpesvirus lytic replication. Virology 266:17–25. https://doi.org/10.1006/viro.1999.0077.
7. Arvanitakis L, Yaseen N, Sharma S. 1995. Latent membrane protein-1 induces cyclin D2 expression, pRb hyperphosphorylation, and loss of TGF-beta 1-mediated growth inhibition in EBV-positive B cells. J Immunol 155:1047–1056.
8. Li M, Lee H, Yoon DW, Albrecht JC, Fleckenstein B, Neipel F, Jung JU. 1997. Kaposi's sarcoma-associated herpesvirus encodes a functional cyclin. J Virol 71:1984–1991.
9. Chang Y, Moore PS, Talbot SJ, Boshoff CH, Zarkowska T, Godden-Kent Paterson H, Weiss RA, Mittnacht S. 1996. Cyclin encoded by KS herpesvirus. Nature 382:410–410. https://doi.org/10.1038/382410a0.
10. van Dyk LF, Virgin HW, Speck SH. 2000. The murine gammaherpesvirus 68 v-cyclin is a critical regulator of reactivation from latency. J Virol 74:7451–7461. https://doi.org/10.1128/JVI.74.16.7451-7461.2000.
11. Hoge AT, Hendrickson SB, Burns WH. 2000. Murine gammaherpesvirus 68 cyclin D homologue is required for efficient reactivation from latency. J Virol 74:7016–7023. https://doi.org/10.1128/JVI.74.15.7016-7023.2000.
12. Gangappa S, van Dyk LF, Jewett TJ, Speck SH, Virgin HW. 2002. Identification of the in vivo role of a viral bcl-2. J Exp Med 195:931–940. https://doi.org/10.1084/jem.20011825.
13. van Dyk LF, Virgin HW, Speck SH. 2003. Maintenance of gammaherpesvirus latency requires viral cyclin in the absence of B lymphocytes. J Virol 77:5118–5126. https://doi.org/10.1128/JVI.77.9.5118-5126.2003.
14. Lee KS, Suarez AL, Claypool DJ, Armstrong TK, Buckingham EM, van Dyk LF. 2012. Viral cyclins mediate separate phases of infection by integrating functions of distinct mammalian cyclins. PLoS Pathog 8:e1002496. https://doi.org/10.1371/journal.ppat.1002496.
15. Williams LM, Niemeyer BF, Franklin DS, Clambey ET, van Dyk LF. 2015. A conserved gammaherpesvirus cyclin specifically bypasses host p18 INK4c to promote reactivation from latency. J Virol 89:10821–10831. https://doi.org/10.1128/JVI.00891-15.
16. Tourigny MR, Ursini-Siegel J, Lee H, Toellner K-M, Cunningham AF, Franklin DS, Ely S, Chen M, Qin X-F, Xiong Y, MacLennan ICM, Chen-Kiang S. 2002. CDK inhibitor p18INK4c is required for the generation of functional plasma cells. Immunity 17:179–189. https://doi.org/10.1016/S1074-7613(02)00364-3.
17. Jeffrey PD, Tong L, Pavletich NP. 2000. Structural basis of inhibition of CDK-cyclin complexes by INK4 inhibitors. Genes Dev 14:3115–3125. https://doi.org/10.1101/gad.851100.
18. Hirai H, Roussel MF, Kato JY, Ashmun RA, Sherr CJ. 1995. Novel INK4 proteins, p19 and p18, are specific inhibitors of the cyclin D-dependent kinases CDK4 and CDK6. Mol Cell Biol 15:2672–2681. https://doi.org/10.1128/MCB.15.5.2672.
19. Nealy MS, Coleman CB, Li H, Tibbetts SA. 2010. Use of a virus-encoded enzymatic marker reveals that a stable fraction of memory B cells expresses latency-associated nuclear antigen throughout chronic gammaherpesvirus infection. J Virol 84:7523–7534. https://doi.org/10.1128/JVI.02572-09.
20. Diebel KW, Oko LM, Medina EM, Niemeyer BF, Warren CJ, Claypool DJ, Tibbetts SA, Cool CD, Clambey ET, van Dyk LF. 2015. Gammaherpesvirus small noncoding RNAs are bifunctional elements that regulate infection and contribute to virulence in vivo. mBio 6:e01670-14. https://doi.org/10.1128/mBio.01670-14.
21. Tibbetts SA, van Dyk LF, Speck SH, Virgin HW. 2002. Immune control of the number and reactivation phenotype of cells latently infected with a gammaherpesvirus. J Virol 76:7125–7132. https://doi.org/10.1128/JVI.76.14.7125-7132.2002.
22. Coleman CB, Nealy MS, Tibbetts SA. 2010. Immature and transitional B cells are latency reservoirs for a gammaherpesvirus. J Virol 84:13045–13052. https://doi.org/10.1128/JVI.01455-10.
23. Weck KE, Kim SS, Virgin HW, IV, Speck SH. 1999. Macrophages are the major reservoir of latent murine gammaherpesvirus 68 in peritoneal cells. J Virol 73:3273–3283.
24. Flaño E, Husain SM, Sample JT, Woodland DL, Blackman MA. 2000. Latent murine γ-herpesvirus infection is established in activated B cells, dendritic cells, and macrophages. J Immunol 165:1074–1081.
25. Weck KE, Kim SS, Virgin HW, IV, Speck SH. 1999. B cells regulate murine gammaherpesvirus 68 latency. J Virol 73:4651–4661.
26. Rekow MM, Darrah EJ, Mboko WP, Lange PT, Tarakanova VL. 2016. Gammaherpesvirus targets peritoneal B-1 B cells for long-term latency. Virology 492:140–144. https://doi.org/10.1016/j.virol.2016.02.022.
27. Lee KS, Cool CD, van Dyk LF. 2009. Murine gammaherpesvirus 68 infection of gamma interferon-deficient mice on a BALB/c background results in acute lethal pneumonia that is dependent on specific viral genes. J Virol 83:11397–11401. https://doi.org/10.1128/JVI.00989-09.
28. Lee KS, Groshong SD, Cool CD, Kleinschmidt-DeMasters BK, van Dyk LF. 2009. Murine gammaherpesvirus 68 infection of IFNgamma unresponsive mice: a small animal model for gammaherpesvirus-associated B-cell lymphoproliferative disease. Cancer Res 69:5481–5489. https://doi.org/10.1158/0008-5472.CAN-09-0291.
29. Tarakanova VL, Kreisel F, White DW, Virgin HW. 2008. Murine gammaherpesvirus 68 genes both induce and suppress lymphoproliferative disease. J Virol 82:1034–1039. https://doi.org/10.1128/JVI.01426-07.
30. Mandal P, Krueger BE, Oldenburg D, Andry KA, Beard RS, White DW, Barton ES. 2011. A gammaherpesvirus cooperates with interferon-alpha/beta-induced IRF2 to halt viral replication, control reactivation, and minimize host lethality. PLoS Pathog 7:e1002371. https://doi.org/10.1371/journal.ppat.1002371.
31. Feldman ER, Kara M, Coleman CB, Grau KR, Oko LM, Krueger BJ, Renne R, van Dyk LF, Tibbetts SA. 2014. Virus-encoded microRNAs facilitate gammaherpesvirus latency and pathogenesis in vivo. mBio 5:e00981-14. https://doi.org/10.1128/mBio.00981-14.
32. Steed AL, Barton ES, Tibbetts SA, Popkin DL, Lutzke ML, Rochford R, Virgin HW. 2006. Gamma interferon blocks gammaherpesvirus reactivation from latency. J Virol 80:192–200. https://doi.org/10.1128/JVI.80.1.192-200.2006.
33. Steed A, Buch T, Waisman A, Virgin HW. 2007. Gamma interferon blocks

gammaherpesvirus reactivation from latency in a cell type-specific manner. J Virol 81:6134–6140. https://doi.org/10.1128/JVI.00108-07.
34. Li Q, Zhou F, Ye F, Gao S-J. 2008. Genetic disruption of KSHV major latent nuclear antigen LANA enhances viral lytic transcriptional program. Virology 379:234–244. https://doi.org/10.1016/j.virol.2008.06.043.
35. Forrest JC, Paden CR, Allen RD, Collins J, Speck SH. 2007. ORF73-null murine gammaherpesvirus 68 reveals roles for mLANA and p53 in virus replication. J Virol 81:11957–11971. https://doi.org/10.1128/JVI.00111-07.
36. Ballestas ME, Chatis PA, Kaye KM. 1999. Efficient persistence of extrachromosomal KSHV DNA mediated by latency-associated nuclear antigen. Science 284:641–644. https://doi.org/10.1126/science.284.5414.641.
37. Upton JW, van Dyk LF, Speck SH. 2005. Characterization of murine gammaherpesvirus 68 v-cyclin interactions with cellular cdks. Virology 341:271–283. https://doi.org/10.1016/j.virol.2005.07.014.
38. Upton JW, Speck SH. 2006. Evidence for CDK-dependent and CDK-independent functions of the murine gammaherpesvirus 68 v-cyclin. J Virol 80:11946–11959. https://doi.org/10.1128/JVI.01722-06.
39. Lim S, Kaldis P. 2013. Cdks, cyclins and CKIs: roles beyond cell cycle regulation. Development 140:3079–3093. https://doi.org/10.1242/dev.091744.
40. Xie X-Q, Yang P, Zhang Y, Zhang P, Wang L, Ding Y, Yang M, Tong Q, Cheng H, Ji Q, McGuire T, Yuan W, Cheng T, Gao Y. 2015. Discovery of novel INK4C small-molecule inhibitors to promote human and murine hematopoietic stem cell ex vivo expansion. Sci Rep 5:18115. https://doi.org/10.1038/srep18115.
41. Gao Y, Yang P, Shen H, Yu H, Song X, Zhang L, Zhang P, Cheng H, Xie Z, Hao S, Dong F, Ma S, Ji Q, Bartlow P, Ding Y, Wang L, Liu H, Li Y, Cheng H, Miao W, Yuan W, Yuan Y, Cheng T, Xie X-Q. 2015. Small-molecule inhibitors targeting INK4 protein p18(INK4C) enhance ex vivo expansion of haematopoietic stem cells. Nat Commun 6:6328. https://doi.org/10.1038/ncomms7328.
42. Yokota T, Matsuzaki Y, Sakai T. 2004. Trichostatin A activates p18INK4c gene: differential activation and cooperation with p19INK4d gene. FEBS Lett 574:171–175. https://doi.org/10.1016/j.febslet.2004.08.025.
43. Sánchez-Aguilera A, Delgado J, Camacho FI, Sánchez-Beato M, Sánchez L, Montalbán C, Fresno MF, Martín C, Piris MA, García JF. 2004. Silencing of the p18INK4c gene by promoter hypermethylation in Reed-Sternberg cells in Hodgkin lymphomas. Blood 103:2351–2357. https://doi.org/10.1182/blood-2003-07-2356.
44. Styles CT, Bazot Q, Parker GA, White RE, Paschos K, Allday MJ. 2017. EBV epigenetically suppresses the B cell-to-plasma cell differentiation pathway while establishing long-term latency. PLoS Biol 15:e2001992-30. https://doi.org/10.1371/journal.pbio.2001992.
45. Weck KE, Barkon ML, Yoo LI, Speck SH, Virgin HWIV. 1996. Mature B cells are required for acute splenic infection, but not for establishment of latency, by murine gammaherpesvirus 68. J Virol 70:6775–6780.
46. Tischer BK, Smith GA, Osterrieder N. 2010. En passant mutagenesis: a two step markerless red recombination system, p 421–430. *In* In vitro mutagenesis protocols. Humana Press. Totowa, NJ.
47. Adler H, Messerle M, Koszinowski UH. 2001. Virus reconstituted from infectious bacterial artificial chromosome (BAC)-cloned murine gammaherpesvirus 68 acquires wild-type properties in vivo only after excision of BAC vector sequences. J Virol 75:5692–5696. https://doi.org/10.1128/JVI.75.12.5692-5696.2001.
48. Gierasch WW, Zimmerman DL, Ward SL, VanHeyningen TK, Romine JD, Leib DA. 2006. Construction and characterization of bacterial artificial chromosomes containing HSV-1 strains 17 and KOS. J Virol Methods 135:197–206. https://doi.org/10.1016/j.jviromet.2006.03.014.
49. Franklin DS, Godfrey VL, Lee H, Kovalev GI, Schoonhoven R, Chen-Kiang S, Su L, Xiong Y. 1998. CDK inhibitors p18(INK4c) and p27(Kip1) mediate two separate pathways to collaboratively suppress pituitary tumorigenesis. Genes Dev 12:2899–2911. https://doi.org/10.1101/gad.12.18.2899.
50. Michaud F, Coulombe F, Gaudreault É, Kriz J, Gosselin J. 2010. Involvement of TLR2 in recognition of acute gammaherpesvirus-68 infection. PLoS One 5:e13742. https://doi.org/10.1371/journal.pone.0013742.
51. Nguyen Y, McGuffie BA, Anderson VE, Weinberg JB. 2008. Gammaherpesvirus modulation of mouse adenovirus type 1 pathogenesis. Virology 380:182–190. https://doi.org/10.1016/j.virol.2008.07.031.
52. Coomes SM, Farmen S, Wilke CA, Laouar Y, Moore BB. 2011. Severe gammaherpesvirus-induced pneumonitis and fibrosis in syngeneic bone marrow transplant mice is related to effects of transforming growth factor-β. Am J Pathol 179:2382–2396. https://doi.org/10.1016/j.ajpath.2011.08.002.